THE JOURNAL OF PHYSICAL CHEMISTRY A
Cite This: J. Phys. Chem. A XXXX, XXX, XXX-XXX
Article
pubs.acs.org/JPCA

Electric Dipole–Magnetic Dipole Polarizability and Anapole Magnetizability of Hydrogen Peroxide as Functions of the HOOH Dihedral Angle

S. Pelloni,[†] P. F. Provasi,[‡] G. I. Pagola,[§] M. B. Ferraro,[§] and P. Lazzeretti*[,∥]

[†]Polo agroindustriale di Parma c/o I.T.I.S. Galileo Galilei, Via Martiri di Cefalonia 14, S. Secondo, 43126 Parma, Italy
[‡]Departamento de Física, Northeastern University, Av. Libertad 5500, W3400 AAS Corrientes, Argentina
[§]Departamento de Física, Facultad de Ciencias Exactas y Naturales and IFIBA, CONICET, Universidad de Buenos Aires, Ciudad Universitaria, Pab. I, 1428 Buenos Aires, Argentina
[∥]Istituto di Struttura della Materia, Consiglio Nazionale delle Ricerche, Via del Fosso del Cavaliere 100, 00133 Roma, Italy

ABSTRACT: The trace of tensors that account for chiroptical response of the H_2O_2 molecule is a function of the HO–OH dihedral angle. It vanishes at 0° and 180°, due to the presence of molecular symmetry planes, but also for values in the range 90–100° of this angle, in which the molecule is unquestionably chiral. Such an atypical effect is caused by counterbalancing contributions of diagonal tensor components with nearly maximal magnitude but opposite sign, determined by electron flow in open or closed helical paths, and associated with induced electric and magnetic dipole moments and anapole moments. For values of dihedral angle external to the 90–100° interval, the helical paths become smaller in size, thus reducing the amount of cancellation among diagonal components. Shrinking of helical paths determines the appearance of extremum values of tensor traces approximately at 50° and 140° dihedral angles.

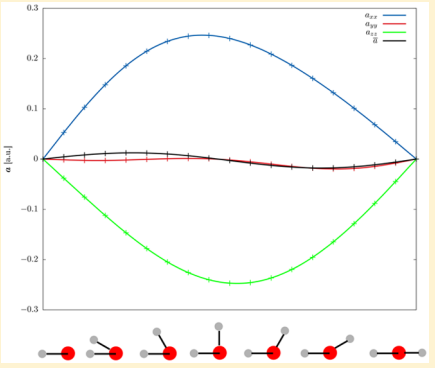

1. INTRODUCTION

After some earlier observations of Hougen,[1,2] Longuet-Higgins proposed the idea of feasible permutations and permutation-inversions, which may be achieved without passage over a high potential barrier, for semirigid molecules, and argued that practicable operations form groups which could be interpreted as the molecular groups of both rigid and nonrigid molecules.[3,4]

In the light of the arguments raised by Longuet-Higgins[3] and of further investigations,[5−8] the hydrogen peroxide molecule, H_2O_2, could not be regarded as a chiral system. Actually, free rotation about the O–O internuclear axis precludes separation of enantiomers in the gas phase, or in solution, at room temperature. However, the existence of a hindering potential permits us to define a preferred equilibrium configuration as that energetically more stable.

Values given in an early study by Hunt et al.[9] for *trans* and *cis* potential barrier heights are 386 and 2460 cm^{-1}, respectively; the potential-function minima are located 111.5° from the *cis* configuration and the activation energy for interconversion through the *trans* configuration is 4617.6 J mol^{-1}. In an accurate *ab initio* study on the equilibrium structure and torsional potential energy function of hydrogen peroxide, Koput[10] reported V_{trans} = 377 cm^{-1} and V_{cis} = 2545 cm^{-1}.

However, hydrogen peroxide is considered by many theoreticians to be an archetypal example of *axial chirality*, which, for systems not possessing a stereogenic center, refers to stereoisomerism resulting from the nonplanar arrangement of substituent groups—ordered according to the Cahn–Ingold–Prelog priority rules (atoms in the case of H_2O_2) about a *chiral axis*.[11]

The configurations in axially chiral systems are specified using the stereochemical labels R_a or S_a: the chiral axis is viewed end-on and the sense of either configuration is identified as that of the clockwise or anticlockwise rotation of a group (the H atom of an OH bond for H_2O_2), starting with the end of the molecule that is closest, then finishing with the end that is farthest.

An alternative designation, *P* (plus) or *M* (minus), is based on the *helicity* of a configuration, because an axially chiral structure is characterized by a helical, i.e., screw-shaped, geometry. Accordingly, *P*, or Δ, is used for a right-handed helix, whereas *M*, or Λ, is used for a left-handed helix. These labels are displayed in Figure 1 to distinguish the enantiomers of hydrogen peroxide.

Some typical properties of H_2O_2, e.g., electric dipole–magnetic dipole polarizability, related to the optical rotatory dispersion (ORD),[12,13] isotropic polarizability of proton nuclear magnetic shielding,[14] and parity violation energy,[15,16] have been studied as functions of the dihedral angle between the OH bonds.

A common feature of the curves reported is that, as expected, each property vanishes for values 0° and 180° of the dihedral

Received: September 12, 2017
Revised: October 22, 2017
Published: November 13, 2017

DOI: 10.1021/acs.jpca.7b09104
J. Phys. Chem. A XXXX, XXX, XXX–XXX

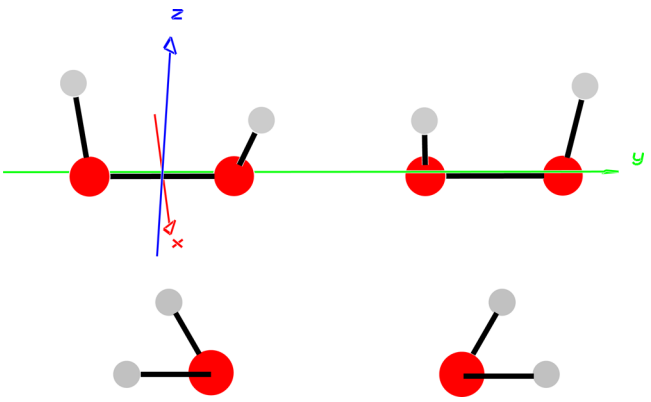

Figure 1. *M* (on the right) and *P* (on the left) enantiomers of the hydrogen peroxide molecule, also denoted as R_a and S_a, respectively, according to an alternative nomenclature, with the subscript "a" referring to "axially chiral".[11]

angle, corresponding to C_{2v} and C_{2h} point-group symmetries, characterized by the presence of a σ_v' and σ_h molecular symmetry planes. However, another recurring feature is constituted by a null value of these properties evaluated in the proximity of 90°, which cannot be related to the existence of pseudorotations: that conformation is by all means chiral. The analogous distinctive characteristic has been reported also for H_2S_2.[17]

To the best of our knowledge, the reasons for the presence of this additional vanishing value of chiroptical properties of H_2O_2 has not been explained. The present paper attempts to interpret the results found for the electric dipole−magnetic dipole polarizability and for the anapole magnetizability, which is a peculiar quantity characterizing chiral molecules in the presence of magnetic field.[18−23]

2. THEORETICAL BACKGROUND

Standard tensor formalism is employed, e.g., the Einstein convention of implicit summation over two repeated Greek subscripts is in force. The third-rank Levi−Civita pseudotensor is indicated by $\epsilon_{\alpha\beta\gamma}$. The SI units are used throughout.

Electronic operators are denoted by boldface letters, e.g., for the electric and magnetic dipoles,[12,13,23]

$$\hat{\boldsymbol{\mu}} = -e\hat{\boldsymbol{R}} \tag{1}$$

$$\hat{\boldsymbol{m}} = -\frac{e}{2m_e}\hat{\boldsymbol{L}} \tag{2}$$

using capitals for global electronic operators, e.g., for position and angular momentum,

$$\hat{\boldsymbol{R}} = \sum_{k=1}^{n} \boldsymbol{r}_k \qquad \hat{\boldsymbol{L}} = \sum_{k=1}^{n} \hat{\mathbf{l}}_k$$

or specifying the vector components, e.g., for the anapole operator,[20]

$$\hat{a}_\alpha = -\frac{1}{2}\epsilon_{\alpha\beta\gamma}\hat{m}_{\beta\gamma} = \frac{e}{6m_e}\sum_{k=1}^{n}[(r^2\delta_{\alpha\beta} - r_\alpha r_\beta)\hat{p}_\beta + i\hbar r_\alpha]_k \tag{3}$$

related to that for the magnetic quadrupole,[24,25]

$$\hat{m}_{\alpha\beta} = -\frac{e}{6m_e}\sum_{k=1}^{n}(\hat{l}_\alpha r_\beta + r_\beta \hat{l}_\alpha)_k \tag{4}$$

The mixed electric dipole−magnetic dipole polarizability is defined by the nonsymmetric parity-odd, time-even, second-rank tensor[12,13,22,23]

$$\kappa'_{\alpha\beta} = -\frac{1}{\hbar}\sum_{j\neq a}\frac{2\omega}{\omega_{ja}^{\ 2} - \omega^2}\mathcal{I}(\langle a|\hat{\mu}_\alpha|j\rangle\langle j|\hat{m}_\beta|a\rangle) \tag{5}$$

The anapole magnetizability $a_{\alpha\beta}$ is also a nonsymmetric parity-odd, time-even, second-rank tensor,[18−23] characterized by striking analogies with $\kappa'_{\alpha\beta}$. It is given by the sum of paramagnetic and diamagnetic contributions,

$$a_{\alpha\beta} = a^{\mathrm{p}}_{\alpha\beta} + a^{\mathrm{d}}_{\alpha\beta} \tag{6}$$

$$a^{\mathrm{p}}_{\alpha\beta} = \frac{1}{\hbar}\sum_{j\neq a}\frac{2}{\omega_{ja}}\mathcal{R}(\langle a|\hat{a}_\alpha|j\rangle\langle j|\hat{m}_\beta|a\rangle) \tag{7}$$

$$a^{\mathrm{d}}_{\alpha\beta} = \frac{e^2}{12m_e}\epsilon_{\alpha\beta\gamma}\langle a|\sum_{k=1}^{n}(r^2 r_\gamma)_k|a\rangle \tag{8}$$

One can at once verify, from eqs 7 and 8, that the average anapole magnetizability contains only the paramagnetic contribution, i.e.,

$$\bar{a} = (1/3)a_{\alpha\alpha} \equiv (1/3)a^{\mathrm{p}}_{\alpha\alpha} \tag{9}$$

because $a^{\mathrm{d}}_{\alpha\alpha}$ vanishes identically.

The sum rule[23] arrived at by summing the terms in the numerator of eq 7,

$$\sum_{j\neq a}\mathcal{R}(\langle a|\hat{a}_\alpha|j\rangle\langle j|\hat{m}_\alpha|a\rangle) = 0 \tag{10}$$

corresponds to the Condon sum rule[26] for rotational strengths R_{aj},

$$\sum_{j\neq a}R_{aj} = \sum_{j\neq a}\mathcal{I}(\langle a|\hat{\mu}_\alpha|j\rangle\langle j|\hat{m}_\alpha|a\rangle) = 0 \tag{11}$$

Because the molecular response properties defined by eqs 5 and 6 are accounted for by second-rank tensors that are not symmetric under the exchange of the indices, it is useful to divide them[23,27−32] into three parts. For any nonsymmetric $T_{\alpha\beta}$ tensor one can write

$$T_{\alpha\beta} = \bar{T}\delta_{\alpha\beta} + \Sigma_{\alpha\beta} + \epsilon_{\alpha\beta\gamma}T^*_\gamma \tag{12}$$

$$\bar{T} = \frac{1}{3}T_{\alpha\alpha} \tag{13}$$

$$\Sigma_{\alpha\beta} = S_{\alpha\beta} - \bar{S}\delta_{\alpha\beta} \qquad \bar{S} = \frac{1}{3}S_{\alpha\alpha} = \bar{T} \tag{14}$$

$$S_{\alpha\beta} = \frac{1}{2}(T_{\alpha\beta} + T_{\beta\alpha}) \tag{15}$$

$$T^*_\gamma = \frac{1}{2}\epsilon_{\gamma\delta\epsilon}T_{\delta\epsilon} \tag{16}$$

where the different terms are referred to as

- $T_{\alpha\alpha}$, trace,
- $\bar{T}\delta_{\alpha\beta}$, isotropic (or spherical) part,
- $\Sigma_{\alpha\beta}$, symmetric traceless anisotropic part (or deviator[33]),
- $\epsilon_{\alpha\beta\gamma}T^*_\gamma = \frac{1}{2}(T_{\alpha\beta} - T_{\beta\alpha})$, antisymmetric part.

The same terminology (deviator, *etc.*) was employed recently by Tomassini et al.[34] in the definition of Raman optical activity

DOI: 10.1021/acs.jpca.7b09104
J. Phys. Chem. A XXXX, XXX, XXX−XXX

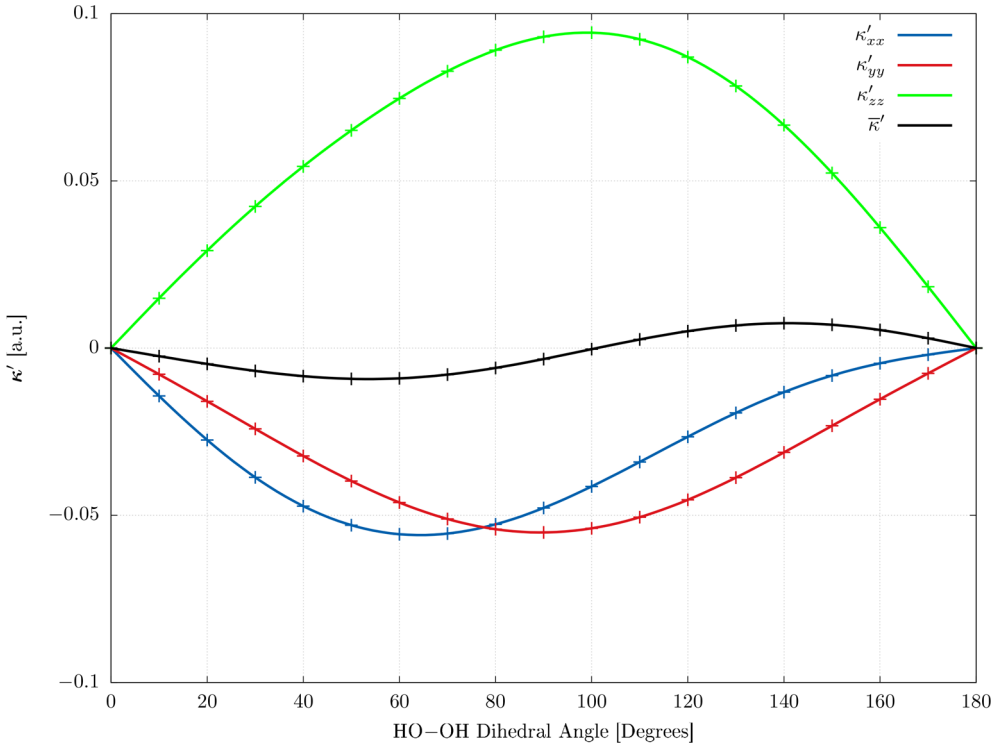

Figure 2. Diagonal components κ'_{xx}, κ'_{yy}, κ'_{zz} and average $\overline{\kappa}' = \kappa'_{\alpha\alpha}/3$, in au, of the electric dipole−magnetic dipole polarizability, eq 5, of the *P* enantiomer of hydrogen peroxide molecule as functions of the HO−OH dihedral angle, computed at the B3LYP level for the frequency ω = 0.0773571 au, equivalent to 3.198×10^{15} rad s^{-1} and $\lambda = 5.890 \times 10^{-7}$ m, corresponding to the sodium D line. Here and in the following Figures 3−6, the curves have been obtained by fitting 19 equally spaced points in the range 0°−180° of dihedral angle, which increases by an anticlockwise rotation from C_{2v} (with both OH bonds along the positive *z* axis) to C_{2h} point-group symmetry. From the CODATA compilation,[50] the conversion factors from au to SI units are for angular frequency $E_h/\hbar = 4.134\,137\,333\,656 \times 10^{16}$ rad s^{-1}; for mixed electric-magnetic dipole polarizability $e^2a_0^3/\hbar = 3.607\ \ 015\,63 \times 10^{-35}$ m C $T^{-1} \equiv$ m kg^{-1} s C^2 per molecule.

(ROA) robustness parameters. The connection between robustness angles and dissymmetry factors in vibrational circular dichroism (VCD) spectra has been dealt with in a more recent paper.[35,36]

The symmetric **S** matrix has real eigenvalues $\mathbf{s} = \mathbf{U}^t\mathbf{S}\mathbf{U}$ and orthogonal eigenvectors **U**. Through simple calculations one obtains

$$\mathrm{Tr}\,\mathbf{\Sigma}^2 = \sum_{i=1}^{3} (s_i - \overline{S})^2 \tag{17}$$

$$= \sum_{i=1}^{3} (s_i^2 - \overline{S}^2) \tag{18}$$

$$= \frac{1}{3}[(s_1 - s_2)^2 + (s_2 - s_3)^2 + (s_3 - s_1)^2] \tag{19}$$

$$= \mathrm{Tr}\,\mathbf{S}^2 - \frac{1}{3}(\mathrm{Tr}\,\mathbf{S})^2 \equiv (\Delta S)^2 \tag{20}$$

Equations 17−20 define the *magnitude of the anisotropy of the deviator*, which is the same as

$$(\Delta S)^2 = \frac{1}{3}[(T_{xx} - T_{yy})^2 + (T_{yy} - T_{zz})^2 + (T_{zz} - T_{xx})^2] + \frac{1}{2}[(T_{xy} + T_{yx})^2 + (T_{yz} + T_{zy})^2 + (T_{zx} + T_{xz})^2] \tag{21}$$

The relationship

$$\Delta S = \sqrt{\mathrm{Tr}\,\mathbf{\Sigma}^2} \tag{22}$$

defines the *anisotropy of the deviatoric part* of a nonsymmetric $T_{\alpha\beta}$ tensor. The square root, ΔS, of the right-hand side in eq 22 is frequently used to designate the anisotropy of a symmetric $S_{\alpha\beta}$ tensor.[37−42]

From eq 17 one obtains the definitions of *variance* dividing by 3, and of *standard deviation of the eigenvalues from the mean* $\overline{S}$,

$$\sigma = \sqrt{\frac{1}{3}\sum_{i=1}^{3} (s_i - \overline{S})^2} \tag{23}$$

Accordingly, eq 23 specifies a measure of variation of the eigenvalues of the symmetric part of a nonsymmetric tensor from its average value: a small (large) σ (or ΔS) indicates that the eigenvalues s_i are close to (distant from) the mean $\overline{S}$.

Relationships 17−20 and 21 and 22 define absolute quantities, independent of the arbitrary coordinate systems used to represent $T_{\alpha\beta}$ and of the index of eigenvalues and eigenvectors.

An alternative definition of anisotropy of a nonsymmetric tensor, given by

$$\Delta T = T_{zz} - \frac{1}{2}(T_{xx} + T_{yy}) \equiv S_{zz} - \frac{1}{2}(S_{xx} + S_{yy}) \tag{24}$$

is sometimes used.[43] At variance with definition (22), its magnitude and sign depend on the coordinate system chosen, which, in our opinion, makes the former, eq 22, preferable.

DOI: 10.1021/acs.jpca.7b09104
J. Phys. Chem. A XXXX, XXX, XXX−XXX

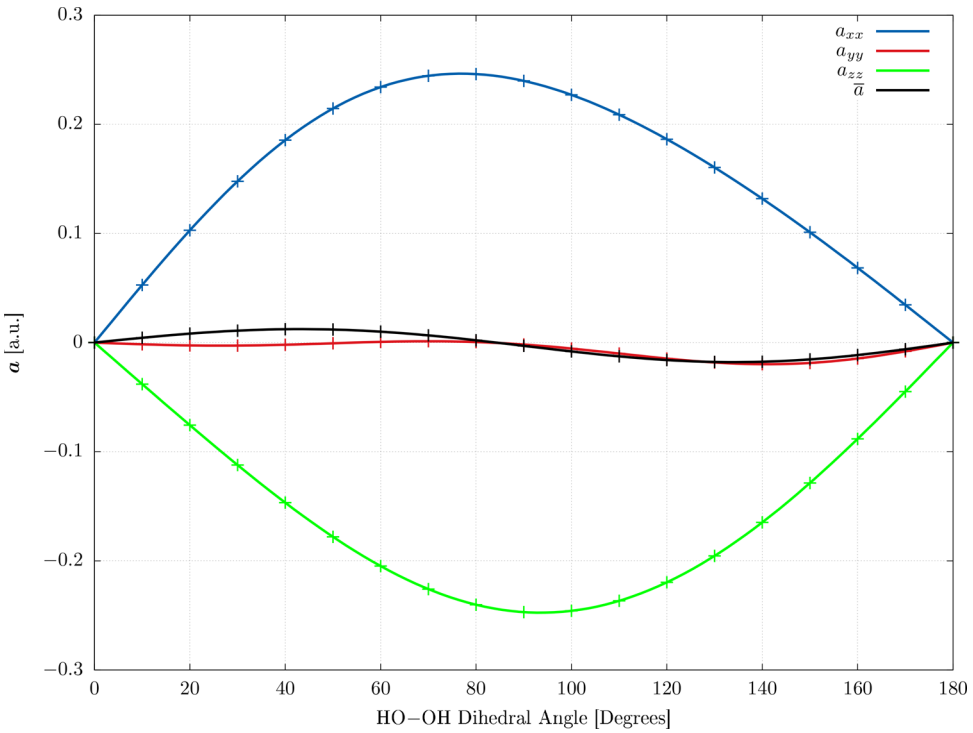

Figure 3. Diagonal components a_{xx}, a_{yy}, a_{zz} and average $\overline{a} = a_{\alpha\alpha}/3$ of the anapole magnetizability, eq 6, in au, of the *P* enantiomer of hydrogen peroxide molecule as functions of the HO−OH dihedral angle, computed at the CCSD level. From the CODATA compilation,[50] the conversion factor from au to SI units per molecule for anapole magnetizabilities is $e^2a_0{}^3/m_e = 4.175\,756\,62 \times 10^{-39}$ J T^{-2} m.

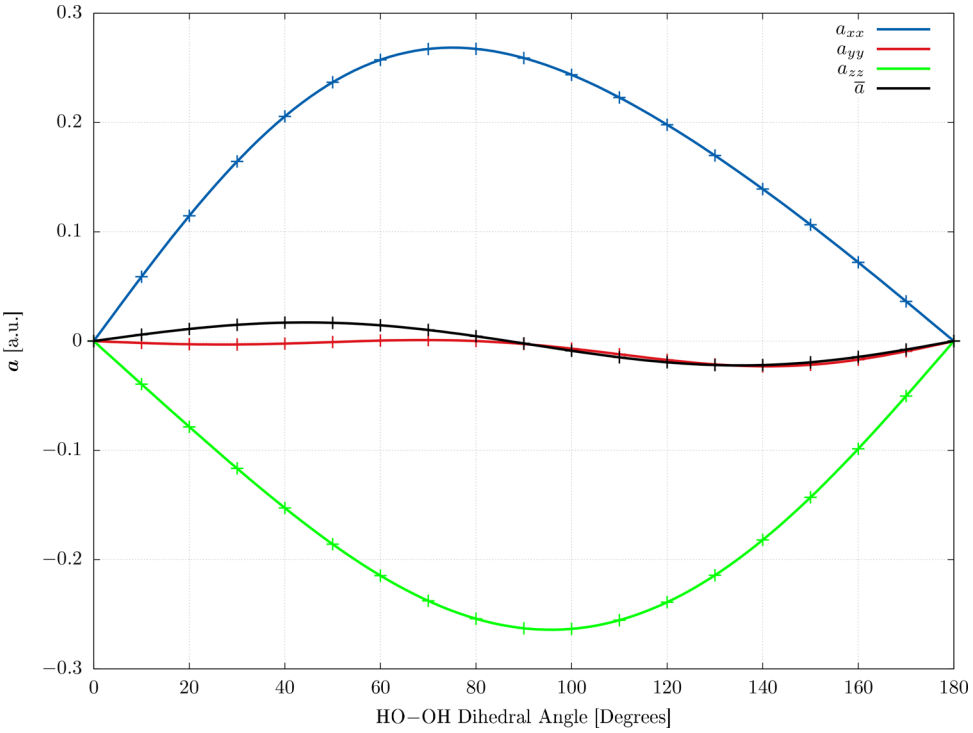

Figure 4. Diagonal components a_{xx}, a_{yy}, a_{zz} and average $\overline{a} = a_{\alpha\alpha}/3$, in au, of the anapole magnetizabiity of the *P* enantiomer of the hydrogen peroxide molecule as functions of the HO−OH dihedral angle computed at the B3LYP level. See the caption to Figure 3 for the conversion factor to SI units.

3. COMPUTATIONS

The equilibrium geometry of the H_2O_2 molecule was optimized at the B3LYP[44] level of accuracy via the GAUSSIAN code.[45] A large uncontracted (13s10p5d2f/11s7p4d) basis set, previously tested for predicting anapole magnetizabilities of $C_4H_4O_2$ cyclic molecules,[20] and other chiral molecules,[21] has been employed to compute electric dipole−magnetic dipole polarizability and anapole magnetizability for 19 molecular conformations corresponding to different values of the HO−OH dihedral angle, using the DALTON code.[46]

DOI: 10.1021/acs.jpca.7b09104
J. Phys. Chem. A XXXX, XXX, XXX−XXX

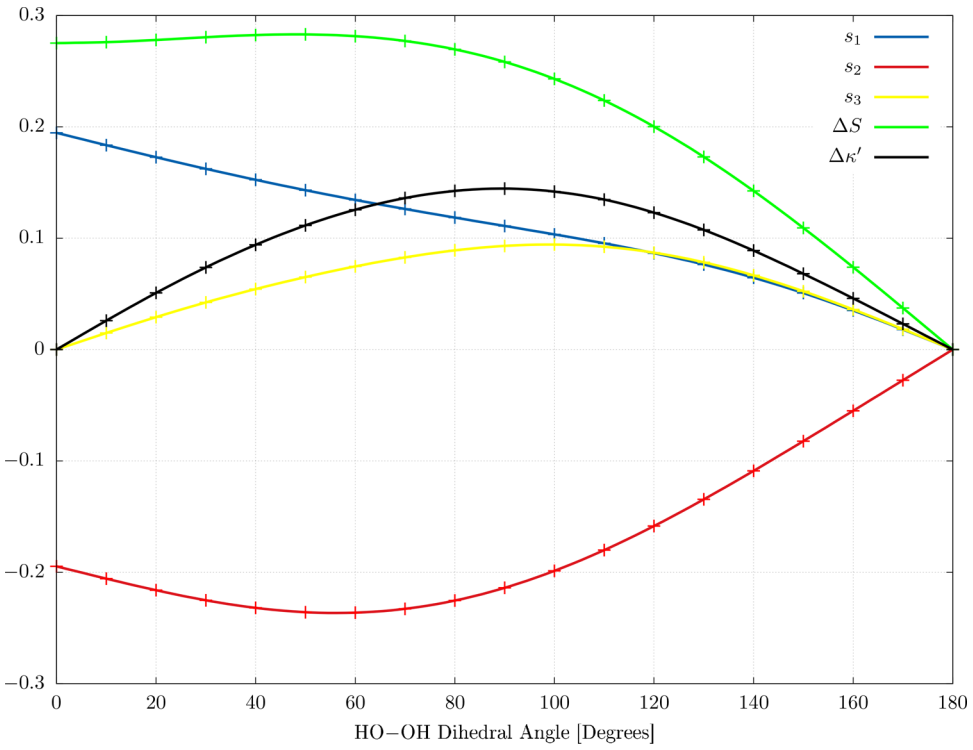

Figure 5. Parameters quantifying the anisotropy of the $\boldsymbol{\kappa}'$ tensor of the *P* enantiomer of the hydrogen peroxide molecule as functions of the dihedral angle of HO−OH computed at the B3LYP level, for the frequency $\omega = 0.077\,357\,1$ au. The conventional anisotropy $\Delta\kappa' = \kappa'_{zz} - (1/2)(\kappa'_{xx} + \kappa'_{yy})$ is represented in black, and the eigenvalues s_1, s_2, and s_3 of the symmetric part, eq 15, are represented in blue, red, and yellow, respectively. The anisotropy defined via eq 22 is represented in green. For conversion factors, see the caption to Figure 2.

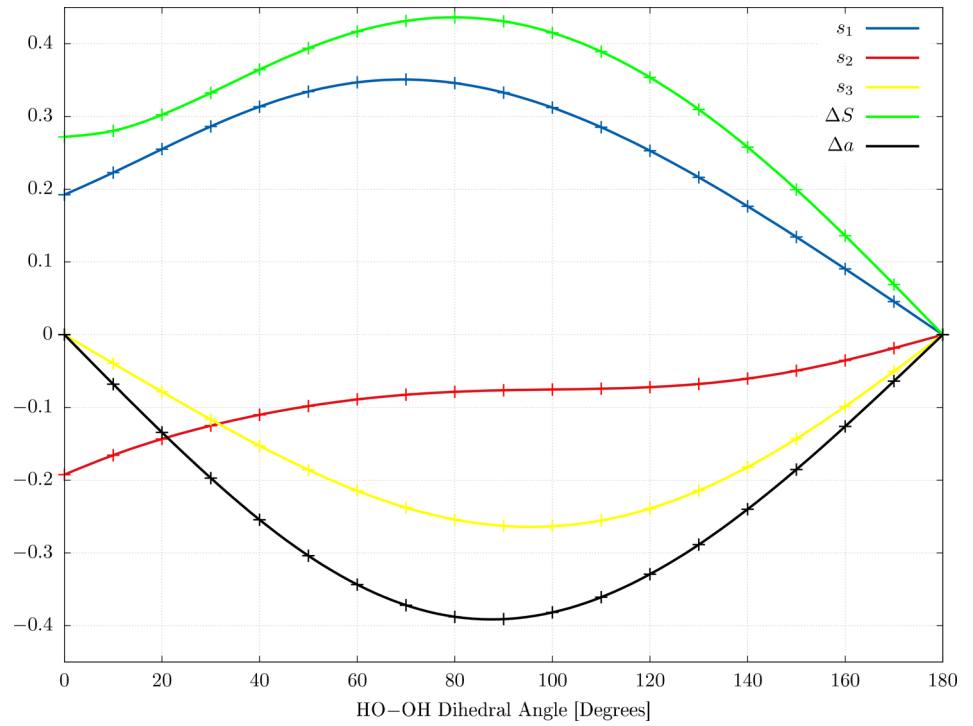

Figure 6. Parameters quantifying the anisotropy of the $\boldsymbol{a}$ tensor of the hydrogen peroxide molecule as functions of the HO−OH dihedral angle computed at the B3LYP level. The conventional anisotropy $\Delta a = a_{zz} - (1/2)\,(a_{xx} + a_{yy})$ is represented in black, and the eigenvalues s_1, s_2, and s_3 of the symmetric part, eq 15, are represented in blue, red, and yellow, respectively. The anisotropy defined via eq 22 is represented in green. For the conversion factor, see the caption to Figure 3.

Calculations of the molecular tensors, eqs 5, 7, and 8, have been carried out at the coupled SCF-HF level of accuracy, equivalent to the random-phase approximation (RPA).[47] The effects of electron correlation have been estimated via density

DOI: 10.1021/acs.jpca.7b09104
J. Phys. Chem. A XXXX, XXX, XXX−XXX

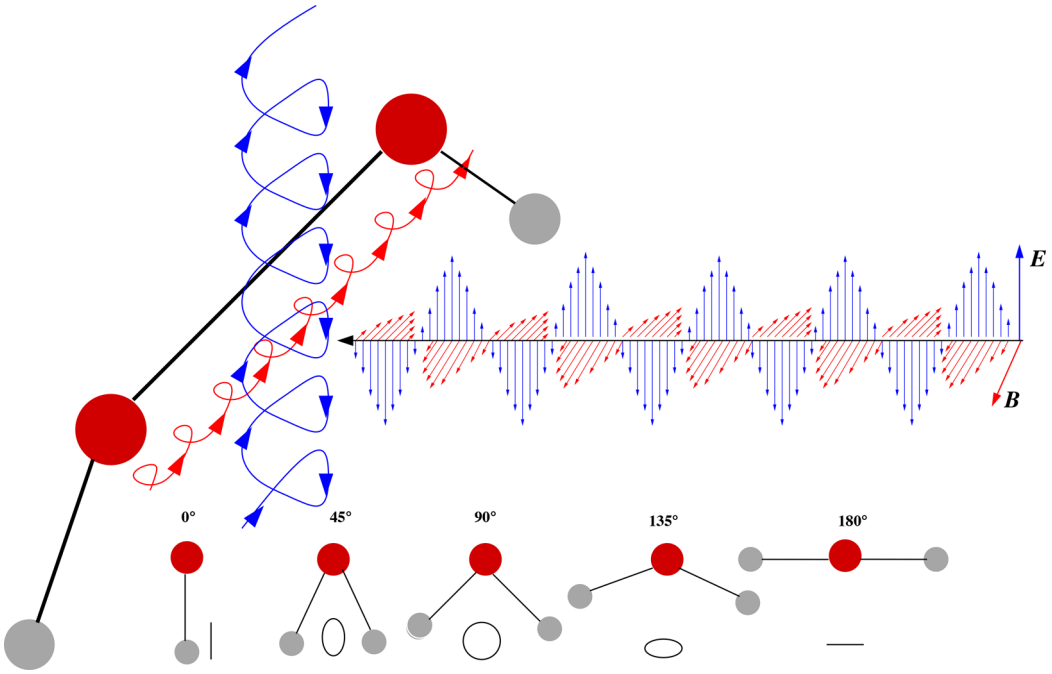

Figure 7. Electrons moving backward and forward along helical paths, under the influence of the fields of a plane-polarized light beam, induce oscillating dipole moments,[48] eqs 25 and 26, determined by the electric dipole−magnetic dipole polarizability, eq 5, of H_2O_2. A section of the helix with axis parallel to the y axis has nearly maximal area for a dihedral HO−OH angle close to 90° and shrinks by increasing or decreasing this value, which reduces the magnitude of κ'_{yy}.

functional theory (DFT), taking into account the B3LYP[44] functional. An attempt at sampling the quality of this functional was made by comparison with coupled cluster singles and doubles (CCSD) computations of anapole magnetizability. Very small differences between beyond Hartree−Fock methods were found, which do not affect the analysis of the following Section.

4. DISCUSSION

Figure 2 shows that the average $\bar{\kappa}' = \kappa'_{\alpha\alpha}/3$ computed at the B3LYP level is significantly smaller than the diagonal components, because they are characterized by different signs. The trace $\kappa'_{\alpha\alpha}$ vanishes for a dihedral angle of ≈100°, which is promptly explained: κ'_{zz} is nearly maximum in the proximity of this value, offsetting κ'_{xx} and κ'_{yy}, which have minima at ≈65° and ≈90°, respectively: they annihilate each other on summing. Consistent with the extremum values of the diagonal components in that range, the anisotropy $\Delta\kappa'$ evaluated via the conventional definition, eq 24, is close to its maximum at ≈90°, as observed in Figure 5.

Analogous patterns are observed for the anapole magnetizability, in the vicinity of 85° and 90°, respectively for the CCSD and B3LYP calculations; see Figures 3 and 4. In particular, the anisotropy Δa from eq 24 is minimum for ≈90°, as shown in Figure 6.

Having found that null average values of chiroptical properties of hydrogen peroxide at a dihedral angle of ≈90° are due to cancellation of contributions with opposite sign of diagonal tensor components, one can conjecture that an analogous effect is likely to take place in *any* axially chiral molecule, e.g., in alkenes with conjugated double bonds, CH_2═CH—CH═CH_2, and biphenyls for a rotation about the central C—C σ bond. Biphenyls with large substituents at the ortho positions on either side of the central C—C are characterized by restricted rotation about it, owing to steric hindrance. If the substituents are different, a chiral biphenyl exists as a pair of axially chiral *atropisomers* that may exhibit features analogous to those observed for H_2O_2.

An explanation can now be found for the existence of extremum values of the diagonal components at ≈90° in the light of perspicuous classical models proposed by Kauzmann.[48] The electrons of chiral molecules in the presence of optical fields move along helical paths; thus let us consider a beam of plane-polarized light propagating in the x direction, impinging on the H_2O_2 molecule represented in Figure 1. The time-dependent electric field E_z, Figure 7, induces an oscillating magnetic moment in a spiralling path, assimilated to a solenoid, whose axis lies in the same direction.[48] It is determined by the time derivative $\dot{E}_z$ of the electric field via the κ'_{zz} component of the electric dipole−magnetic dipole polarizability,[12,13,37]

$$\Delta\langle\hat{m}_z\rangle = -\kappa'_{zz}\dot{E}_z\omega^{-1} \tag{25}$$

Analogously, the magnetic field B_y of the polarized wave induces an electric dipole moment[48] in a coil spiralling about an axis parallel to the y axis; see Figures 1 and 7.[12,13,37]

$$\Delta\langle\hat{\mu}_y\rangle = \kappa'_{yy}\dot{B}_y\omega^{-1} \tag{26}$$

Plane-polarized light beams shone in the y and z directions will induce electric and magnetic dipoles in a similar way. Now, the mechanism magnifying the absolute value of the diagonal components of $\boldsymbol{\kappa}'$ in the vicinity of a dihedral angle of 90° is seen to depend on the shape and size of the helical path observed in the direction of its axis. In the bottom of Figure 7 the shrinking of a section of circular helix with axis parallel to the y axis, corresponding to 90°, is displayed for increasing or decreasing values of the dihedral angle. An analogous mechanism is expected to shrink the vertical helix and taper

DOI: 10.1021/acs.jpca.7b09104
J. Phys. Chem. A XXXX, XXX, XXX−XXX

off κ'_{zz}. Light beams shone along the z or x axis would determine a similar phenomenology.

Figures 3 for CCSD and 4 for B3LYP calculations, displaying components and average value of the anapole magnetizability as functions of the HO−OH dihedral angle, are characterized by features similar to those observed for $\boldsymbol{\kappa}'$, i.e., vanishing $\overline{a}$ and extremum values of the a_{xx} and a_{zz} components at angles close to 90°. Remarkably, the a_{yy} component is much smaller than the others, and comparatively less affected by a change of dihedral angle.

To interpret this effect, one can tentatively assume that a magnetic field B_y induces a toroidal flow about the y axis, and consequently an anapole moment[18,23] in that direction, as found for dithiins.[49] The magnitude of this anapole moment is much smaller than that of the anapole moments in the x and z directions, according to Figures 3 and 4. In any event, further investigations and plots of magnetic-field induced current densities are needed to visually check this hypothesis.

To understand the value of the definition of tensor anisotropy relying on eq 22, let us examine Figure 5, which illustrates the dependence of the eigenvalues of the symmetric part of the $\kappa'_{\alpha\beta}$ tensor on the HO−OH dihedral angle. The largest value of the eigenvalue s_1 is found at 0°, i.e., for the C_{2v} molecular symmetry. It diminishes quite smoothly on increasing the angle, and it vanishes together with s_2 (with a minimum at ≈60°) and s_3 (with a maximum at ≈100°) at 180°, i.e., for the C_{2h} symmetry.

Whereas the anisotropy $\Delta\kappa'$ designated via eq 24 vanishes at 0° and 180°, passing through a maximum at ≈90°, the anisotropy ΔS defined by eq 22, giving a measure of the dispersion of the eigenvalues s_i from the mean $\overline{S}$, is quite large in the interval 0−60°; then it diminishes, vanishing together with the eigenvalues at 180°.

At the ends of the range of dihedral angles considered in Figure 2 for the $\boldsymbol{\kappa}'$ tensor, $T_{xx} = T_{yy} = T_{zz} = S_{xx} = S_{yy} = S_{zz} = \overline{S} = 0$, and because the trace of the $\mathbf{S}$ matrix is conserved on diagonalizing, $\overline{S} = s_1 + s_2 + s_3 = 0$ at 0° and 180°. Because s_3 also vanishes at the ends, Figure 5, then either $s_2 = -s_1$ at 0° or $s_1 = s_2 = 0$ at 180°, as shown in the same figure. An analogous pattern is observed for the anapole magnetizability in Figures 4 and 6. The curve representing the eigenvalue s_2 as a function of the dihedral angle passes through a saddle point in the proximity of 90°, where s_3 and Δa reach a minimum value. The eigenvalue s_1 and the anisotropy ΔS have a maximum at ≈70° and ≈80°, respectively.

These results provide more detailed and reliable information on the intrinsic anisotropy of chiroptical tensors than definition (24).

5. CONCLUDING REMARKS

Accurate beyond Hartree−Fock calculations show that the average value $\overline{\kappa}'$ of the electric dipole−magnetic dipole polarizability tensor of hydrogen peroxide, formally related to its optical rotatory power (whose observation is, however, precluded by free rotation about the O−O bond), vanishes in a configuration close to that of equilbrium geometry, corresponding to a dihedral HO−OH angle ≈100°, at which the molecule is certainly chiral.

This third point of vanishing rotatory power, in addition to those occurring at 0° and 180°, which correspond to C_{2v} and C_{2h} point-group symmetries, respectively, does not depend on the existence of pseudorotations, e.g., symmetry planes. Analogous results, observed previously for other tensor properties typical of axially chiral molecules (as well as for the scalar parity-violation energy), were found also for the average anapole magnetizability of H_2O_2.

The present investigations demonstrate that these additional points of vanishing tensor trace are due to mutual cancellation of diagonal components with opposite sign, characterized by extremum values in the range ≈65−100° of the dihedral angle, at which tensor anisotropies, evaluated via two definitions, also have nearly maximal magnitude.

However, extremum values of diagonal components are physically explained in terms of open helical paths of electrons for the electric dipole−magnetic dipole polarizability and of closed helical paths, i.e., toroidal flow, for the anapole magnetizability. The magnitude of the diagonal components of chiroptical tensors depends on the shape and size of these paths: they shrink by increasing or decreasing the dihedral angle ≈100°, which corresponds to the maximum calculated values.

Analogous effects, in particular the presence of additional vanishing average values of chiroptical tensors, are expected to take place for other axially chiral molecules, e.g., atropisomers. Eventually, because ORD and ROA are intimately connected, the approach adopted in the present study would be useful also in other contexts, e.g., theoretical prediction of ROA parameters as functions of the dihedral angle in axially chiral systems.

AUTHOR INFORMATION

Corresponding Author

*P. Lazzeretti. E-mail: lazzeret@gmail.com.

ORCID

P. Lazzeretti: 0000-0001-9595-1180

Notes

The authors declare no competing financial interest.

ACKNOWLEDGMENTS

Financial support from CONICET, Northeastern University and Universidad de Buenos Aires are gratefully acknowledged.

REFERENCES

(1) Hougen, J. T. Classification of rotational energy levels for symmetric-top molecules. *J. Chem. Phys.* **1962**, *37* (7), 1433−1441.

(2) Hougen, Jon T. Classification of rotational energy levels. II. *J. Chem. Phys.* **1963**, *39* (2), 358−365.

(3) Longuet-Higgins, H. C. The symmetry groups of non-rigid molecules. *Mol. Phys.* **1963**, *6* (06), 445−460.

(4) Longuet-Higgins, H. C. The symmetry groups of non-rigid molecules. *Mol. Phys.* **2002**, *100* (01), 11−20.

(5) Watson, J. K. G. On the symmetry groups of non-rigid molecules. *Mol. Phys.* **1971**, *21*, 577−585.

(6) Gilles, J.-M. F.; Philippot, J. Internal symmetry groups of non-rigid molecules. *Int. J. Quantum Chem.* **1972**, *6*, 225−261.

(7) Russell, D. K. The symmetry groups of non-rigid molecules: a Lie algebraic and group contraction approach. *Mol. Phys.* **1998**, *93* (02), 441−455.

(8) Watson, J. K. G. Simplification of the molecular vibration-rotation hamiltonian. *Mol. Phys.* **2002**, *100* (1), 47−54.

(9) Hunt, Robert H.; Leacock, Robert A.; Peters, C. Wilbur; T. Hecht, Karl Internal rotation in hydrogen peroxide: The far-infrared spectrum and the determination of the hindering potential. *J. Chem. Phys.* **1965**, *42* (6), 1931−1946.

(10) Koput, Jacek An ab initio study on the equilibrium structure and torsional potential energy function of hydrogen peroxide. *Chem. Phys. Lett.* **1995**, *236* (4), 516−520.

DOI: 10.1021/acs.jpca.7b09104
J. Phys. Chem. A XXXX, XXX, XXX−XXX

(11) International Union of Pure and Applied Chemistry Compendium of Chemical Terminology Gold Book, Version 2.3.3 2014-02−24 https://goldbook.iupac.org/pdf/goldbook.pdf.
(12) Lazzeretti, P. Electric and magnetic properties of molecules. In *Handbook of Molecular Physics and Quantum Chemistry*; Wilson, S., Ed.; John Wiley & Sons, Ltd.: Chichester, 2003; Vol. 3 Part 1, Chapter 3, pp 53−145..
(13) Ligabue, A.; Lazzeretti, P.; Béccar Varela, M. P.; Ferraro, M. B. On the resolution of the optical rotatory power of chiral molecules into atomic terms. A study of hydrogen peroxide. *J. Chem. Phys.* **2002**, *116* (15), 6427−6434.
(14) Buckingham, A. D. Chirality in NMR spectroscopy. *Chem. Phys. Lett.* **2004**, *398*, 1−5.
(15) Lazzeretti, P.; Zanasi, R. On the calculation of parity-violating energies in hydrogen peroxide and hydrogen disulphide molecules within the random-phase approximation. *Chem. Phys. Lett.* **1997**, *279*, 349−354.
(16) Hennum, A. C.; Helgaker, T.; Klopper, W. Parity-violating interaction in H_2O_2 calculated from density-functional theory. *Chem. Phys. Lett.* **2002**, *354* (3−4), 274−282.
(17) Pericou-Cayere, Marjorie; Rerat, Michel; Dargelos, Alain Theoretical treatment of the electronic circular dichroism spectrum and the optical rotatory power of H_2S_2. *Chem. Phys.* **1998**, *226* (3), 297−306.
(18) Provasi, P. F.; Pagola, G. I.; Ferraro, M. B.; Pelloni, S.; Lazzeretti, P. Magnetizabilities of diatomic and linear triatomic molecules in a time-independent nonuniform magnetic field. *J. Phys. Chem. A* **2014**, *118*, 6333−6342.
(19) Tellgren, Erik I.; Fliegl, Heike Non-perturbative treatment of molecules in linear magnetic fields: Calculation of anapole susceptibilities. *J. Chem. Phys.* **2013**, *139*, 164118.
(20) Pagola, G. I.; Ferraro, M. B.; Provasi, P. F.; Pelloni, S.; Lazzeretti, P. Theoretical estimates of the anapole magnetizabilities of $C_4H_4X_2$ cyclic molecules for X = O, S, Se, and Te. *J. Chem. Phys.* **2014**, *141* (9), 094305.
(21) Zarycz, Natalia; Provasi, Patricio F; Pagola, Gabriel I; Ferraro, Marta B; Pelloni, Stefano; Lazzeretti, Paolo Computational study of basis set and electron correlation effects on anapole magnetizabilities of chiral molecules. *J. Comput. Chem.* **2016**, *37*, 1552−1558.
(22) Lazzeretti, Paolo The abstract G_{PT} and G_{CPT} groups of discrete *C*, *P* and *T* symmetries. *J. Mol. Spectrosc.* **2017**, *337*, 178−184. Spectroscopy and Inter/Intramolecular Dynamics in Honor of Walther Caminati - Part 2.
(23) Lazzeretti, Paolo Chiral discrimination in nuclear magnetic resonance spectroscopy. *J. Phys.: Condens. Matter* **2017**, *29* (44), 443001.
(24) Lazzeretti, P. Magnetic properties of a molecule in non-uniform magnetic field. *Theor. Chim. Acta* **1993**, *87* (1/2), 59−73.
(25) Faglioni, F.; Ligabue, A.; Pelloni, S.; Soncini, A.; Lazzeretti, P. Molecular response to a time-independent non-uniform magnetic field. *Chem. Phys.* **2004**, *304*, 289−299.
(26) Condon, E. U. Theories of optical rotatory power. *Rev. Mod. Phys.* **1937**, *9*, 432−457.
(27) Buckingham, A. D.; Malm, S. M. Asymmetry in the nuclear magnetic shielding tensor. *Mol. Phys.* **1971**, *22* (6), 1127−1130.
(28) Robert, J. B.; Wiesenfeld, L. Magnetic anisotropic interactions of nuclei in condensed matter. *Phys. Rep.* **1982**, *86*, 363−401.
(29) Buckingham, A. D.; Pyykkö, P.; Robert, J. B.; Wiesenfeld, L. Symmetry rules for the indirect nuclear spin-spin coupling tensor revisited. *Mol. Phys.* **1982**, *46* (1), 177−182.
(30) Andrew, E. R.; Farnell, L. F. The effect of macroscopic rotation on anisotropic bilinear spin interactions in solids. *Mol. Phys.* **1968**, *15*, 157.
(31) Buckingham, A. D.; Love, J. Theory of the anisotropy of nuclear spin coupling. *J. Magn. Reson.* **1970**, *2*, 338−351.
(32) Schneider, R. F. Asymmetry in magnetic second-rank tensor quantities. *J. Chem. Phys.* **1968**, *48* (11), 4905−4909.
(33) Spencer, A. J. M. *Continuum Mechanics*; Dover Books on Physics; Dover Publications, 2004; p 88.
(34) Tommasini, Matteo; Longhi, Giovanna; Mazzeo, Giuseppe; Abbate, Sergio; Nieto-Ortega, Belén; Ramírez, Francisco J.; Casado, Juan; López Navarrete, Juan Teodomiro Mode robustness in Raman optical activity. *J. Chem. Theory Comput.* **2014**, *10* (12), 5520−5527.
(35) Longhi, Giovanna; Tommasini, Matteo; Abbate, Sergio; Polavarapu, Prasad L. The connection between robustness angles and dissymmetry factors in vibrational circular dichroism spectra. *Chem. Phys. Lett.* **2015**, *639* (Supplement C), 320−325.
(36) Longhi, Giovanna; Tommasini, Matteo; Abbate, Sergio; Polavarapu, Prasad L. Corrigendum to "the connection between robustness angles and dissymmetry factors in vibrational circular dichroism spectra" [chem. phys. lett. 639 (2015) 320−325]. *Chem. Phys. Lett.* **2016**, *648* (SupplementC), 208.
(37) Barron, L. D. *Molecular Light Scattering and Optical Activity*, second ed.; Cambridge University Press: Cambridge, 2004.
(38) Herzberg, Gerhard. *Molecular Spectra and Molecular Structure II: Infrared and Raman of Polyatomic Molecules*, first ed.; Van Nostrand, 1956. Eq. III.20, p 247.
(39) Stone, Anthony. *The Theory of Intermolecular Forces*. Oxford University Press, second ed., 2013. p 27.
(40) Weickert, Joachim; Hagen, Hans. *Visualization and Processing of Tensor Fields (Mathematics and Visualization)*, first ed.; Springer, 2005.
(41) Basser, Peter J.; Pierpaoli, Carlo Microstructural and physiological features of tissues elucidated by quantitative-diffusion-tensor MRI. *J. Magn. Reson., Ser. B* **1996**, *111*, 209−219.
(42) Herges, Rainer; Daniel, Geuenich Delocalization of electrons in molecules. *J. Phys. Chem. A* **2001**, *105*, 3214−3220.
(43) Flygare, W. H. Magnetic interactions in molecules and an analysis of molecular electronic charge distribution from magnetic parameters. *Chem. Rev.* **1974**, *74* (6), 653−687.
(44) Becke, Axel D. Density-functional termochemistry. III. the role of exact exchange. *J. Chem. Phys.* **1993**, *98* (7), 5648−5652.
(45) Frisch, M. J.; Trucks, G. W.; Schlegel, H. B.; Scuseria, G. E.; Robb, M. A.; Cheeseman, J. R.; Montgomery, J. A., Jr.; Vreven, T.; Kudin, K. N.; Burant, J. C.; Millam, J. M.; Iyengar, S. S.; Tomasi, J.; Barone, V.; Mennucci, B.; Cossi, M.; Scalmani, G.; Rega, N.; Petersson, G. A.; Nakatsuji, H.; Hada, M.; Ehara, M.; Toyota, K.; Fukuda, R.; Hasegawa, J.; Ishida, M.; Nakajima, T.; Honda, Y.; Kitao, O.; Nakai, H.; Klene, M.; Li, X.; Knox, J. E.; Hratchian, H. P.; Cross, J. B.; Bakken, V.; Adamo, C.; Jaramillo, J.; Gomperts, R.; Stratmann, R. E.; Yazyev, O.; Austin, A. J.; Cammi, R.; Pomelli, C.; Ochterski, J. W.; Ayala, P. Y.; Morokuma, K.; Voth, G. A.; Salvador, P.; Dannenberg, J. J.; Zakrzewski, V. G.; Dapprich, S.; Daniels, A. D.; Strain, M. C.; Farkas, O.; Malick, D. K.; Rabuck, A. D.; Raghavachari, K.; Foresman, J. B.; Ortiz, J. V.; Cui, Q.; Baboul, A. G.; Clifford, S.; Cioslowski, J.; Stefanov, B. B.; Liu, G.; Liashenko, A.; Piskorz, P.; Komaromi, I.; Martin, R. L.; Fox, D. J.; Keith, T.; Al-Laham, M. A.; Peng, C. Y.; Nanayakkara, A.; Challacombe, M.; Gill, P. M. W.; Johnson, B.; Chen, W.; Wong, M. W.; Gonzalez, C.; Pople, J. A. *Gaussian 2003*, Revision C.02; Gaussian, Inc.: Wallingford, CT, 2004.
(46) *DALTON, An electronic structure program*, Release 2.0; 2005; http://www.kjemi.uio.no/software/dalton/.
(47) Jørgensen, P.; Simons, J. *Second Quantization-Based Method in Quantum Chemistry*; Academic Press: New York, 1981.
(48) Kauzmann, Walter. *Quantum Chemistry - An Introduction*; Academic Press Inc.: New York, 1957.
(49) Pelloni, S.; Faglioni, F.; Soncini, A.; Ligabue, A.; Lazzeretti, P. Magnetic response of dithiin molecules: is there anti-aromaticity in nature? *Chem. Phys. Lett.* **2003**, *375*, 583−590.
(50) Mohr, Peter J.; Newell, David B.; Taylor, Barry N. CODATA recommended values of the fundamental physical constants: 2014. *Rev. Mod. Phys.* **2016**, *88*, 035009.

DOI: 10.1021/acs.jpca.7b09104
J. Phys. Chem. A XXXX, XXX, XXX−XXX